CONF-831187--15

Neutron Scattering Study of the Magnetic Excitations in Ferromagnetic Iron at High Energy Transfers

C.-K. Loong and J. M. Carpenter
Intense Pulsed Neutron Source Program
Argonne National Laboratory
Argonne, IL 60439

CONF-831187--15

DE84 003552

J. W. Lynn
Department of Physics and Astronomy
University of Maryland
College Park, MD 20742

R. A. Robinson
Physics Division
Los Alamos National Laboratory
Los Alamos, NM 87545

H. A. Mook
Solid State Division
Oak Ridge National Laboratory
Oak Ridge, TN 37830

ABSTRACT

We have measured the spin-wave spectrum of iron by neutron inelastic scattering using the Low-Resolution Medium-Energy Chopper Spectrometer at the Intense Pulsed Neutron Source (IPNS) of the Argonne National Laboratory. Interest focuses on the magnetic excitations at high energy transfers where the spin-wave dispersion relation has not previously been determined. In measurements performed at 10K using a 23-gram single crystal of pure iron, we observed magnetic scattering around the (110) reciprocal lattice point with spin-wave energies from 40 to 160 meV. The spin-waves over the entire range of energy are found to be consistent with an isotropic spin-wave dispersion relation. With the present experimental sensitivity we were unable to observe any band structure effects such as Stoner excitations or optical magnons in this range of wave vector and energy.

INTRODUCTION

The low temperature spin dynamics of band ferromagnets such as iron and nickel is still not completely understood despite considerable efforts both experimentally and theoretically. Calculations of the magnetic excitations are complicated because the effects of the full band structure must be incorporated[1] in the theory of the dynamic susceptibility, while neutron scattering measurements are difficult because the excitation spectrum extends to very high energies. Collins et al[2] made high resolution measurements of the magnons in iron up to energies of $\lesssim$ 70 meV and found that the excitation spectrum was completely isotropic in reduced wave vector $\vec{q}$ over this range. Mook and Nicklow[3] extended these measurements in the [110] direction to about 110 meV in pure iron, while in a large crystal of ^{54}Fe (4% Si) they found a dramatic decrease in the spin wave intensities for E $\gtrsim$ 90 meV. Lynn[4] found a similar decrease in spin wave intensities in a sample of ^{54}Fe (12% Si) for E $\gtrsim$ 120 meV.

We have used the time-of-flight technique at the pulsed spallation neutron source at Argonne National Laboratory to extend the spin wave measurements in pure iron to higher energies ($\sim$ 160 meV). Our data are consistent with an isotropic spin wave dispersion relation, with the intrinsic strength of the scattering monotonically decreasing with increasing energy. No other effects of band structure were observed, in particular no additional structure or excitations were found. However, the strength of the 'optical' spin wave scattering is predicted to be below the present sensitivity of our instrument. With improvements in instrumentation and source intensity expected in the next few years, it should finally be possible to achieve a complete picture of the spin dynamics of iron.

RESULTS AND DISCUSSION

The measurements were performed using the Low-Resolution Medium-Energy Chopper Spectrometer (LRMECS) at the pulsed spallation neutron source of the

Argonne National Laboratory. This neutron source is particularly well-suited for investigating elementary excitations at high energies because the flux of epithermal neutrons is enhanced compared with conventional sources. The sample was a single crystal of pure iron weighing 23 grams and was oriented in the $[1\bar{1}0]$ scattering plane. All measurements were made at a sample temperature of 10K around the (110) reciprocal lattice point where the magnetic scattering is the largest.

Since the details of the IPNS chopper spectrometers have been given elsewhere[5], we shall only give a brief description of the operation here. A phased Fermi chopper produces pulses of monochromatic neutrons which are incident on the sample. The energy and momentum transfer are determined by neutron time-of-flight techniques in 120 detectors. In the present measurements we used incident energies of 200, 300 and 350 meV to explore different regions of energy transfer. The energy resolution in general varies with energy transfers but was approximately 6-8% of the incident neutron energy in the region of interest. Elastic incoherent scattering from a thin plate of vanadium at the above incident neutron energies provided detector calibration and intensity normalization.

For each detector the momentum transfer $\vec{Q}$ and energy transfer E are coupled together so that a detector at a particular scattering angle scans a parabolic locus in $(\vec{Q},E)$ space. If the locus intercepts the scattering surface for magnons or phonons (where energy and wavevector conservation conditions are satisfied for given energy transfer) then scattering will be observed in the detector. For highly dispersive excitations such as the spin waves in iron the scattered intensities in adjacent detectors can be compared at fixed energy transfer. Figure 1a shows the kinematics for such a "scan" at an energy transfer of 116 meV. Each cross depicts the wave vector position for a separate detector. The scattering surface at this energy, denoted by the circle, can be adjusted to intercept the detector loci by rotating the sample to the proper

orientation. Note that in general the scan will not be along any particular symmetry direction of reduced wave vector $\vec{q}$, and in fact is not even linear. Nevertheless the scan will cross the scattering surface and the excitations can be detected. Although scans along high symmetry direction of $\vec{q}$ could, in principle, be arranged by judiciously choosing the incident neutron energy, crystal orientation and detector angles, the operation is quite restricted as compared to the constant energy mode in a triple-axis spectrometer. For a given incident energy and crystal orientation excitations at different energy transfers may be observed as illustrated in Figure 1b.

Figure 2 shows the observed scattering for the experimental configuration explained in Figure 1. The incident neutron energy was 300 meV. The data have been corrected for detector efficiency (as measured by vanadium calibration run) as well as for the variation in instrumental response with energy transfer so that the scattering function $S(\vec{Q},E)$ is shown. Counts in adjacent time channels corresponding to an energy window of 15 meV have been added together to improve statistics. The observed peaks correspond to spin wave excitations, and are in good agreement with the expected dispersion relation extrapolated from lower energies.

If we assume that the spin wave dispersion relation is isotropic then we can plot the magnitudes of the observed peak position at each energy to obtain the spin-wave spectrum given in Figure 3. The solid curve in the Figure shows the result of fitting a dispersion relation of the form

$$E = D|\vec{q}|^2(1 - \beta|\vec{q}|^2) \qquad (1)$$

to the experimental data. From a least-squares analysis we obtained values of 307 ± 15 meV $\mathring{A}^2$ and 0.32 ± 0.1 meV $\mathring{A}^2$ for D and β respectively. These compare favorably with the low temperature values of D = 325 ± 10 meV $\mathring{A}^2$ and β = 0.9 ± 0.1 meV $\mathring{A}^2$ obtained[2,6] from high resolution measurements at lower energies ($E \lesssim 90$ meV) using triple-axis spectrometers. We should point out that the

values of D and β derived from these fits depend to some extent on the range of energies used for fitting purpose, and thus the different values found for β should not be regarded as a discrepancy (see Fig. 3). In principle higher powers of q should be employed to fit the entire measured spin wave dispersion relation, but we do not feel that such an extension is warranted at this time.

Spin wave intensities and linewidths are presently difficult to measure. Nonetheless the present measurements qualitatively show that the strength of the spin wave scattering in the energy range of 40 to 160 meV monotonically decreases with increasing energy. Such an energy dependence of the spin wave intensity is expected from band structure effects in itinerant ferromagnets in contrast to the constant spin wave intensity versus energy given by the Heisenberg model for localized spins. Recent theory[1] also predicted the existence of an "optical" magnon mode at higher energies, with scattering strength considerably smaller than that of the "acoustic" spin-waves at low energies. With the present experimental sensitivity we were unable to observe any additional magnetic excitations. Clearly more studies are needed to clarify the spin wave spectrum of iron in the region of higher energy. We hope that further development in instrumental sensitivity and neutron source intensity in the near future will lead to a more complete understanding of the spin dynamics in itinerant ferromagnetic materials.

ACKNOWLEDGEMENTS

We are grateful to Dr. D. L. Price for many helpful discussions. Work at ANL supported by U. S. Department of Energy, under Contract No. W-31-109-ENG-38. Work at U. of Maryland supported by the NSF, DMR 79-00908. Work at ORNL supported by the Division of Materials Sciences, U. S. Department of Energy under Contract No. W-7405-ENG-26.

REFERENCES

1. J. F. Cooke, J. W. Lynn and H. L. Davis, Phys. Rev. B21, 4118 (1980).

2. M. F. Collins, V. J. Minkiewicz, R. Nathans, L. Passell and G. Shirane, Phys. Rev. 179, 417 (1969). See also G. Shirane, V. J. Minkiewicz and R. Nathans, J. Appl. Phys. 39, 383 (1968).

3. H. A. Mook and R. M. Nicklow, Phys. Rev. B 7, 336 (1973).

4. J. W. Lynn, Phys. Rev. B 11, 2624 (1975).

5. D. L. Price, J. M. Carpenter, C. A. Pelizzari, S. K. Sinha, I. Bresof and G. E. Ostrowski, Proceedings of the Sixth Meeting of the International Collaboration on Advanced Neutron Sources, June 28-July 2, 1982, ANL-82-80, p. 207 (1983).

6. J. W. Lynn (private communication).

FIGURE CAPTIONS

Figure 1 Schematic diagram of the scattering geometry in reciprocal space for scans of constant energy transfer. (a) Each cross depicts the wave vector position at an energy transfer of 116 meV for the available detectors at a particular incident neutron energy and crystal orientation. The magnon scattering surface at this energy is denoted by the circle. Gaps in the chain of crosses occur because detectors did not exist at the corresponding angles. (b) Detector loci and scattering surfaces for energy transfers of 102, 130 and 150 meV. Scattering is observed at the intercept of a detector locus and a scattering surface corresponding to the same energy transfer.

Figure 2 The measured spin-wave scattering function for the constant energy scans explained in Figure 1. The solid curve in (a), (b) and (c) shows the result of fitting Gaussian functions to the measured data. q is the magnitude of the reduced wave vector deduced from the measured peak positions. Only background scattering is observed in (d) since the detector locus does not intercept the scattering surface at E = 150 meV.

Figure 3 Spin-wave spectrum of pure iron at 10K assuming an isotropic spin-wave dispersion relation. Incident neutron energies of 200, 300 and 350 meV have been used to measure the magnetic excitations from 40 to 160 meV. The solid curve shows the results of fitting the dispersion relation given in Eq. (1) to the experimental data in which D and β were found to be approximately 307 and 0.32 meV Å^2. The dashed curve is calculated from Eq. (1) using D = 325 meV Å^2 and β = 0.9 meV Å^2 (Ref. 2,6).

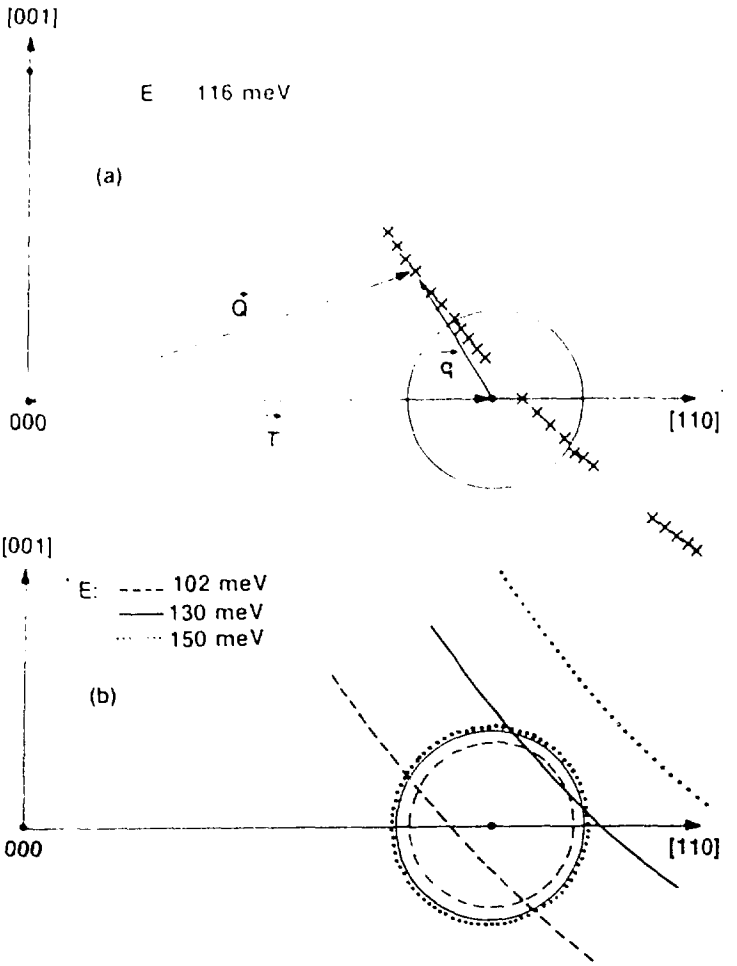

Figure 1 Schematic diagram of the scattering geometry in reciprocal space for scans of constant energy transfer. (a) Each cross depicts the wave vector position at an energy transfer of 116 meV for the available detectors at a particular incident neutron energy and crystal orientation. The magnon scattering surface at this energy is denoted by the circle. Gaps in the chain of crosses occur because detectors did not exist at the corresponding angles. (b) Detector loci and scattering surfaces for energy transfers of 102, 130 and 150 meV. Scattering is observed at the intercept of a detector locus and a scattering surface corresponding to the same energy transfer.

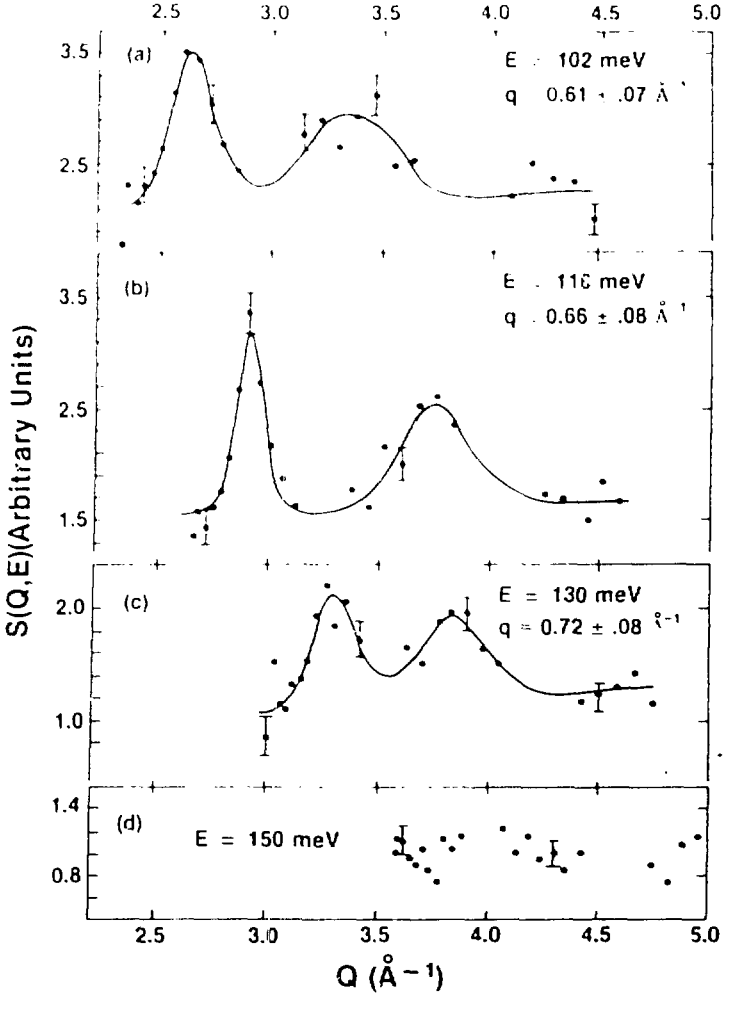

Figure 2 The measured spin-wave scattering function for the constant energy scans explained in Figure 1. The solid curve in (a), (b) and (c) shows the result of fitting Gaussian functions to the measured data. q is the magnitude of the reduced wave vector deduced from the measured peak positions. Only background scattering is observed in (d) since the detector locus does not intercept the scattering surface at E = 150 meV.

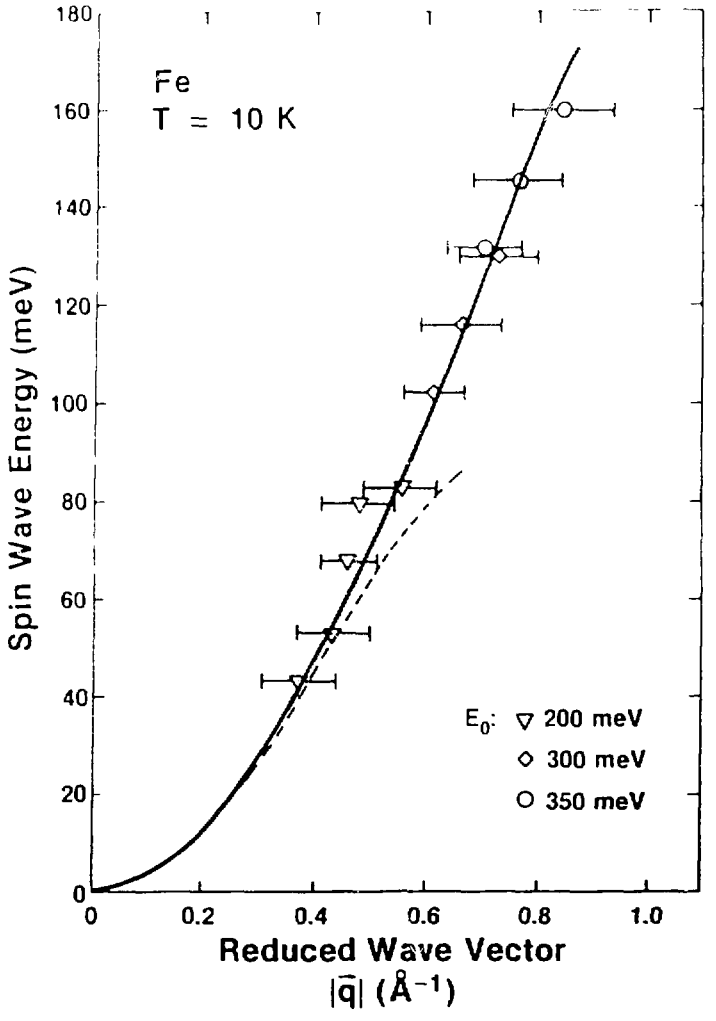

Figure 3 Spin-wave spectrum of pure iron at 10K assuming an isotropic spin-wave dispersion relation. Incident neutron energies of 200, 300 and 350 meV have been used to measure the magnetic excitations from 40 to 160 meV. The solid curve shows the results of fitting the dispersion relation given in Eq. (1) to the experimental data in which D and β were found to be approximately 307 and 0.32 meV Å^2. The dashed curve is calculated from Eq. (1) using D = 325 meV Å^2 and β = 0.9 meV Å^2 (Ref. 2,6).